

Microphase and Macrophase Transitions in Binary Blends of Diblock Copolymers

Hong G. Jeon,[†] Steven D. Hudson,* and Hatsuo Ishida

Department of Macromolecular Science, Case Western Reserve University, Cleveland, Ohio 44106-7202

Steven D. Smith

The Procter and Gamble Company, Cincinnati, Ohio 45239-8707

Received October 26, 1998; Revised Manuscript Received January 11, 1999

ABSTRACT: The macro- and microphase transitions in binary blends of poly(styrene-*b*-isoprene) (SI) and poly(styrene-*b*-ethylenepropylene) (SEP) lamellar diblock copolymers were investigated by optical and electron microscopy and by rheological analysis. A variety of morphologies were produced as a function of blend composition and the rate of solvent evaporation. Numerous morphologies are possible because of the interaction of macro- and microphase separation. As one example, spherical droplets of SEP whose lamellae comprise concentric spherical shells were produced. At the phase boundaries of this and other morphologies, the polystyrene (S) microdomains associated with each phase were in contact. Additional phase separation occurred within the ordered media. When the molecular weight of SI was small and its mobility high, an SI domain was produced at the center of each spherical SEP droplet, thereby reducing the curvature of the SEP lamellae. When the molecular weight of SI was larger and its mobility lower, individual SI lamellae formed within the ordered SEP-rich phase. The solubility of SI in SEP exceeded that of SEP in SI, because of the relative interaction parameters and molecular weights of the copolymers. SI that was dissolved within SEP localized at the microdomain interface and acted to shield the S and EP segments from one another. The lamellar ordering transition of the lower molecular weight SI diblock was determined rheologically. In blends with SEP, the ODT of the SI was increased. This effect was shown to arise from interfacially induced ordering.

Introduction

The ordering transitions of block copolymers and the phase separation of binary polymer blends are well-known. When these two transitions exist in the same system, interesting morphologies are shown here to develop, because the transitions influence one another and their resulting morphologies (see also ref 1). Previous work has identified factors that lead to the miscibility or immiscibility of binary blends of block copolymers or of binary blends of a block copolymer and a homopolymer. In general, consider a binary blend of poly-(A-*b*-B) and poly(C-*b*-D) having respective degree of polymerizations N_{AB} and N_{CD} and volume fraction compositions f_A and f_C . In the mean-field case, the effective interaction parameter between the two polymers is^{2,3}

$$\chi_{\text{eff}} = \chi_{AC}f_Af_C + \chi_{AD}f_Af_D + \chi_{BC}f_Bf_C + \chi_{BD}f_Bf_D - \chi_{AB}f_Af_B - \chi_{CD}f_Cf_D \quad (1)$$

where $f_B = 1 - f_A$ and $f_D = 1 - f_C$. The spinodal condition as a function of the volume fraction of poly(A-*b*-B), ϕ_{AB} , is defined as

$$2(\chi_{\text{eff}})_{\text{spinodal}} = \frac{1}{N_{AB}\phi_{AB}} + \frac{1}{N_{CD}\phi_{CD}} \quad (2)$$

for which the critical point occurs at

[†] Present address: Systran Corporation, Air Force Research Laboratory, Materials Directorate, AFRL/MLBP Building 654, 2941 P Street, Suite 1, Wright-Patterson Air Force Base, OH 45433-7750.

$$\phi_{AB}^* = \frac{1}{1 + \sqrt{N_{AB}/N_{CD}}} \quad \text{and} \quad (\chi_{\text{eff}}N_{\text{eff}})^* = 2 \quad (3)$$

where

$$N_{\text{eff}} = \frac{4N_{AB}N_{CD}}{(\sqrt{N_{AB}} + \sqrt{N_{CD}})^2} \quad (4)$$

Equation 1 is simplified if some of the monomers are identical or if one of the polymers is a homopolymer.

Concerning microphase separation, critical points for pure symmetric polymers in the mean-field limit are $\chi_{AB}N_{AB}$ or $\chi_{CD}N_{CD}$ equal to approximately 10.5.⁴ Non-mean-field effects can increase the critical value of χN for the microphase ordering transition (ODT) considerably.⁵ The mean-field critical points have been calculated numerically for binary blends of block copolymers,⁶ illustrating that the critical value of χN for microphase separation varies smoothly with blend composition.

Experimental investigations have been restricted to two classes. Many studies address binary blends of block copolymers (poly(A-*b*-B)) with homopolymers polyA^{7,8} or polyC.⁹ Mean-field theory (e.g., eqs 1–4) predicts macrophase separation in blends involving block copolymer as well as in blends involving only homopolymers or random copolymers.¹⁰ Other studies address binary blends of block copolymers of the identical chemical structure, but having different composition¹¹ or molecular weight.¹² The latter case illustrates an important feature of the miscibility of copolymer blends: while the effective interaction parameter (eq 1) is zero when the composition of the two copolymers are identical, macrophase separation is observed when the

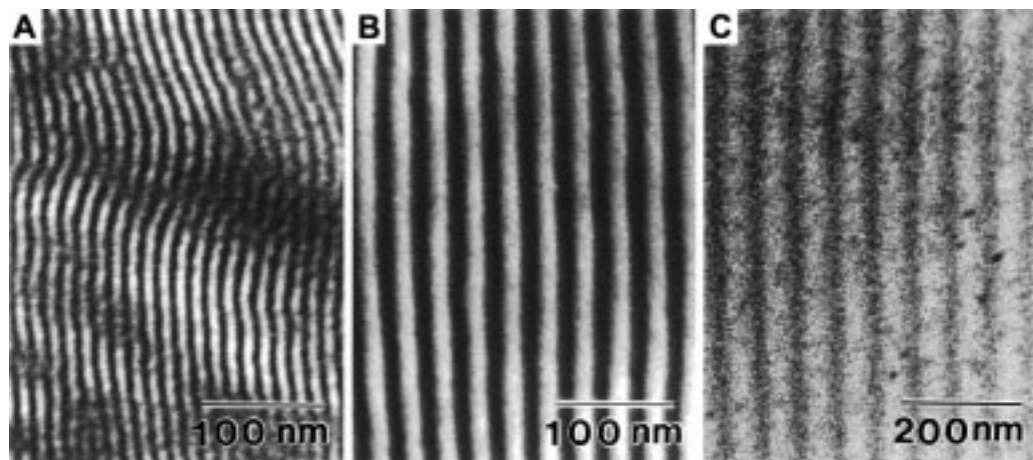


Figure 1. TEM micrographs of neat diblock copolymers showing the equilibrium lamellar structure of (A) SI20, (B) SI100, and (C) SEP110.

molecular weight ratio of the diblock copolymers becomes too large. There is therefore an additional entropic factor that can lead to the phase separation of binary blends of block copolymers, if microphase ordered. This arises from the mismatch in the natural periodicity of the two copolymers. When the molecular weights were within a factor of 5, the copolymers were found to be miscible at all compositions, resulting in a single lamellar phase having a periodicity intermediate between that of the pure components. However, when the molecular weight ratio was larger than 10, the two copolymers phase separated. A considerable amount of low molecular weight copolymer is soluble in the high molecular weight phase, since the low molecular weight polymer can adopt its natural conformation at the microdomain interface, and the higher molecular weight polymer can relax.¹³ However, only a small amount of high molecular weight copolymer can be dissolved in the low molecular weight phase, because of a severe entropic penalty to confine a high molecular weight chain in a small layer spacing.

In this report, we discuss the phase behavior and morphology of binary blends of poly(styrene-*b*-isoprene) (SI) and poly(styrene-*b*-ethylenepropylene) (SEP), i.e., of the type poly(A-*b*-B) and poly(A-*b*-C). We focus on systems that are macrophase separated, forced by the strong incompatibility of styrene and ethylenepropylene segments. We also develop a procedure that we apply in another report¹⁴ to investigate the response of lamellar block copolymer microstructure to an applied shear field.

Experimental Procedure

Monodisperse poly(styrene-*b*-isoprene) diblock copolymers, having weight-average molecular weights equal to ~20 000 (SI20) and 100 000 (SI100) and polydispersity, $M_w/M_n < 1.06$, were synthesized using a standard anionic technique.¹⁵ According to proton NMR, these copolymers had nearly symmetric composition: 52 and 53 wt % PS, respectively. Based upon the relative densities of the segments, the volume fractions of these two copolymers was $f_{S,SI20} = 0.49$ and $f_{S,SI100} = 0.50$. Based upon an equal segment volume of 118 \AA^3 ,¹⁶ the degree of polymerization was $N_{SI20} = 285$ and $N_{SI100} = 1425$. Poly(styrene-*b*-ethylenepropylene) (SEP) diblock (Kraton 1701) was provided by the Shell Chemical Co. The total weight-average molecular weight is 110 000, the weight fraction of PS is 0.37, and the molecular weight polydispersity is ~1.03.¹⁷ Accordingly, $f_{S,SEP} = 0.33$ and $N_{SEP} = 1606$. Each of these diblocks form lamellar ordered phases (see TEM micrographs,

Figure 1). The order-disorder transition (ODT) for pure SI20 is 147 °C. For the other copolymers the ODT is above the decomposition temperature of the respective copolymers. In terms of χN , the most strongly segregated copolymer is SEP110.

SI/SEP blends of various composition were obtained by casting from a dilute (3 wt %) homogeneous solution in toluene, chosen as a nearly nonselective solvent. Under the assumption of nonselectivity,¹⁸

$$\chi_{\text{eff},s} = \chi_{\text{eff}}\phi_p \quad (5)$$

where χ_{eff} is expressed in eq 1 and ϕ_p is the total volume fraction of solids. A small amount (1 wt % relative to the amount of polymer) of antioxidant (Irganox 1010, Ciba Geigy) was added to the solution. Solvent was evaporated very slowly at room temperature during a period of 2 weeks to yield a stabilized structure. The specimens were then annealed at 70 °C under vacuum for 24 h.

Macrophase and microphase transitions during solvent casting were examined in situ by phase-contrast and cross-polarized optical microscopy, respectively. Phase contrast is sensitive to refractive index differences between macrophase of different composition, and cross polars are sensitive to form birefringence arising from lamellar microdomain order. Materials with microphase order therefore produced a birefringent texture. Solutions (10 wt % solids) of blends SEP110 and SI20 were placed between a glass slide and coverslip, and the solvent was allowed to evaporate. The solvent evaporation rate at the edges of the specimen was much faster than within the interior, where 1 or 2 days was required to complete phase separation. Thus, the evaporation rate for the optical microscopy specimens was only slightly faster than for the TEM specimens. Higher resolution examination was done by TEM. Thin sections (~80 nm thickness) were obtained at -100 °C, using an RMC MT-7000 cryomicrotome with a diamond knife. The thin sections were exposed to the vapor of 2% aqueous OsO₄ solutions for 90 min. Bright field images were observed by mass thickness contrast with a JEOL JEM-100CX TEM operated at 100 kV, and as a result of OsO₄ staining, the I, S, and EP microdomains appeared black, gray, and white, respectively. Using these specimen preparation conditions, the image contrast for SI20 and SI100 is greater than that for SEP110. Note that, in all cases, no preferential staining of the interface occurs (Figure 1); rather, the microdomains are stained. This differs from our observations of the blends, reported below.

The ODT of SI20 was measured by a rheological method using a Rheometrics (RMS 800) torsional rheometer with parallel plate geometry. The sample for rheological measurement was compression molded at 130 °C under vacuum to yield a disk with 25 mm diameter and 0.6 mm thickness.

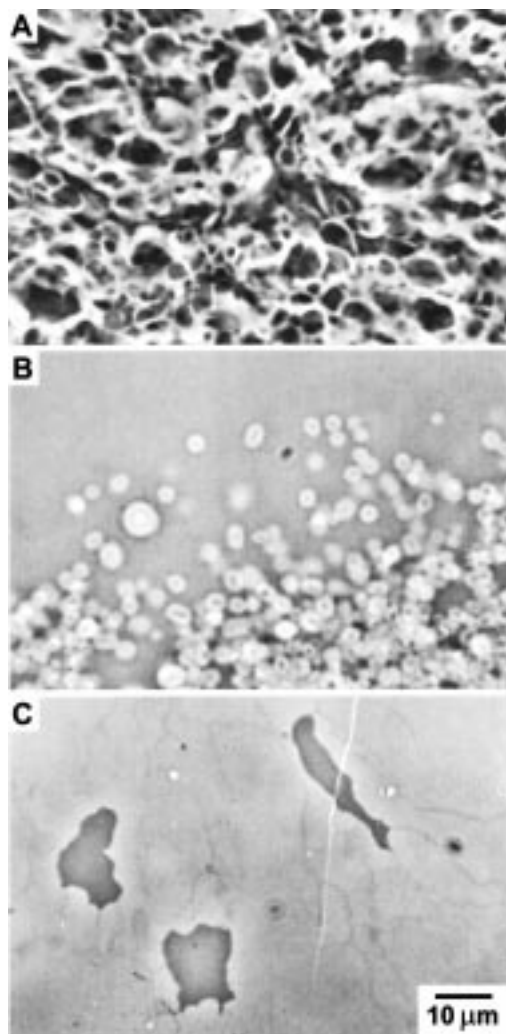


Figure 2. Phase contrast optical micrographs of SI20/SEP110 during solvent evaporation, in which SEP-rich regions appear light. (A) An interconnected morphology observed near the edge of a specimen (containing 80 wt % SI20 and 20 wt % SEP110), where the solvent evaporation rate was rapid, and the structure was formed in several minutes. (B) SEP-rich droplets that have nucleated in a more slowly evaporating section of the specimen shown in (A). The solvent gradient is vertical. As the solvent evaporation continued, droplets appeared in the upper portion of the figure. (C) SI-rich droplets with notched edges in a 50/50 wt % blend.

Results

Macro- and microphase transitions during solvent casting were examined *in situ* by phase-contrast and cross-polarized optical microscopy, respectively. A variety of morphologies ensued depending on blend composition and solvent evaporation rate. Solutions (10 wt % solids) of blends SEP110 and SI20 were placed between a glass slide and coverslip, and the solvent was allowed to evaporate. Near the edges of the specimen, where the solvent evaporation rate was most rapid, interconnected morphologies characteristic of spinodal decomposition were observed (Figure 2A). For blends containing 20 wt % SEP and slightly further from the edge, the morphology that developed upon phase separation was interconnected initially and later evolved to droplets, assumed to be rich in SEP110. In the interior of specimens containing 20 wt % SEP110, where the evaporation proceeded more slowly still, nucleation of SEP-rich droplets was observed (Figure 2B). These droplets grew larger where the evaporation rate was

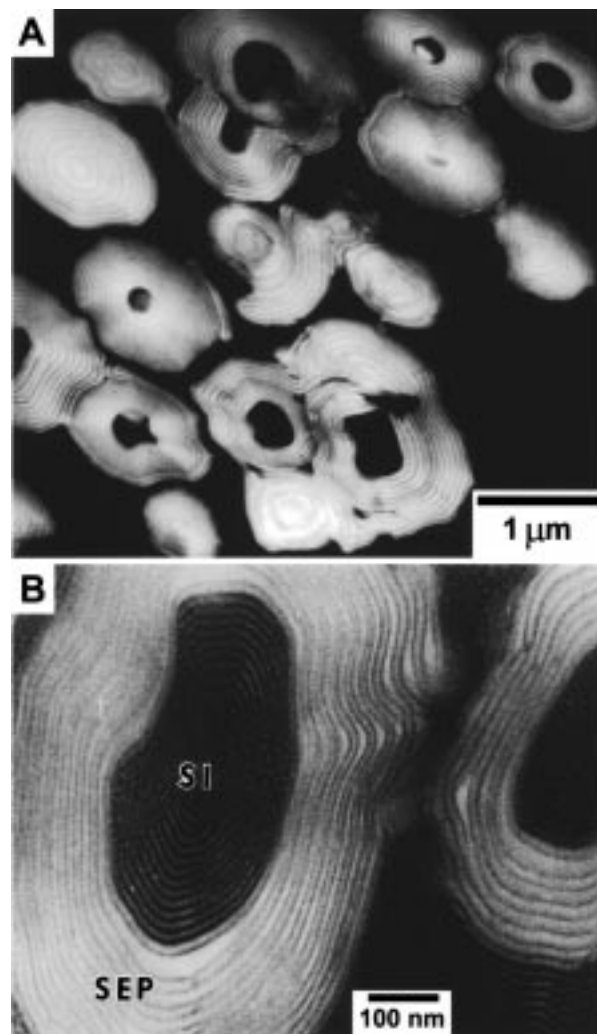


Figure 3. TEM micrographs of SI20/SEP110 (70 wt %/30 wt %) blends. (A) Low magnification image. SEP-rich droplets appear light, and the SI-rich phase is dark. (B) High magnification image.

reduced. Thus, in general terms, the influence of solvent evaporation on the macrodomain morphology was as expected for immiscible polymer blends.

At low concentration of SEP, macrophase separation of SEP-rich droplets and their microphase ordering were more or less simultaneous. At high concentrations of SEP, however, microphase ordering preceded macrophase separation considerably. Subsequent macrophase separation produced droplets with irregularly notched edges (Figure 2C). Similar notched interfaces were also observed in relatively coarse interconnected morphologies. These notches are consistent with the microphase order of the SEP-rich phase. Higher resolution examination of these structures is presented and discussed below (Figure 5).

Sections of the fully dried specimens (20 wt % SEP110 in SI20) examined by TEM reveal that the internal structure of the SEP110 droplets comprises concentric spherical shells (Figure 3A). Moreover, the center of the droplet usually contains SI20, which also adopts a concentric spherical shell morphology. On the basis of optical microscopy (Figure 2B), this core-shell morphology developed almost immediately upon formation of the SEP-rich droplet, perhaps as a result of the concurrent microphase ordering. When the SI core is not found, the apparent lamellar period of the SEP110 is larger at the

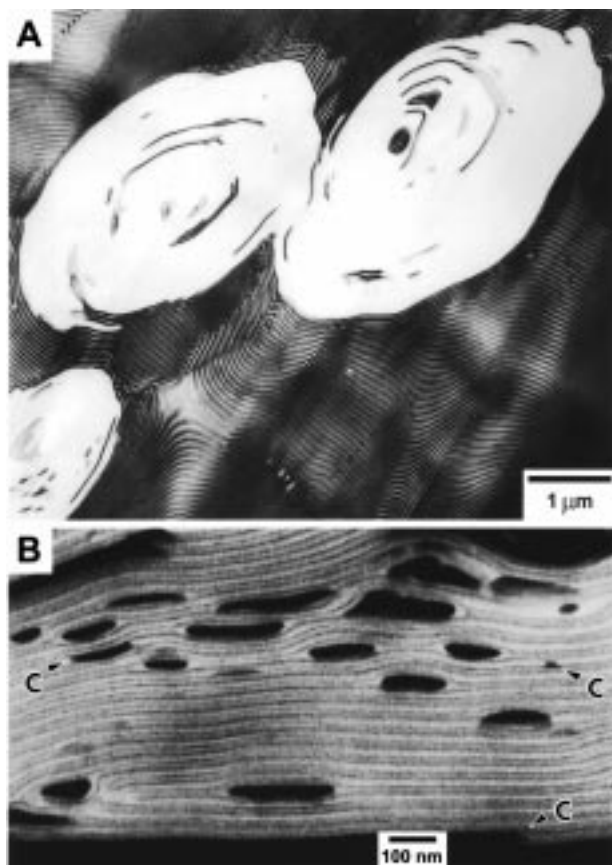


Figure 4. TEM micrographs of SI100/SEP110 (70 wt %/30 wt %) blends: (A) low magnification image; (B) high magnification image.

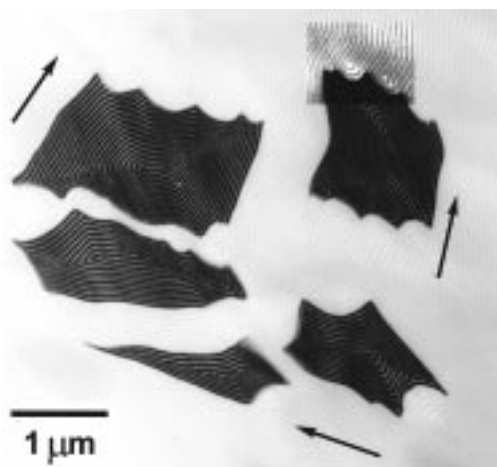


Figure 5. TEM micrograph of SI100/SEP110 (35 wt %/65 wt %) blends. The small rectangular region in the upper right exemplifies a view of the disclinations in the continuous SEP-rich phase, which are responsible for the scalloped shape of the phase boundary.

droplet center, as expected if the section does not pass directly through the center of the droplet.

Higher magnification images (Figure 3B) reveal that lamellae in the SEP110-rich phase do not have the same appearance as pure SEP110 lamellae (Figure 1C). Instead, the lamellae in the SEP110-rich phase have a dark interface. This suggests that SI20 is dissolved within the SEP110-rich phase, where the isoprene segment has been stained dark by OsO_4 .²⁵ The relatively large area fraction of SEP110-rich domains in the images (Figure 2B) is another indication of dissolved

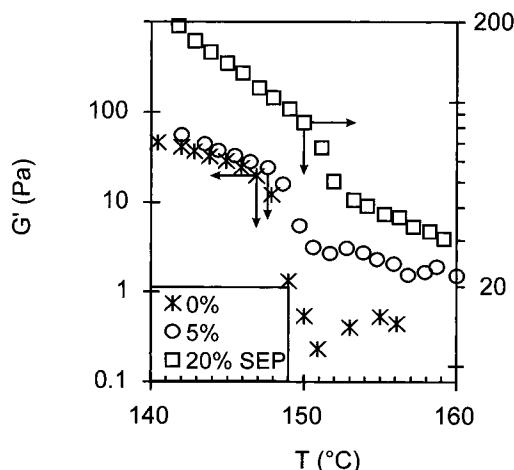


Figure 6. Dynamic elastic modulus of SI20 and its blends with SEP110. The strain amplitude, oscillatory frequency and heating rate were 60%, 1 rad/s, and 1 °C/min, respectively. The left-hand vertical scale corresponds to samples containing 0 and 5 wt %, and the right-hand scale corresponds to the sample containing 20 wt %. The ODT is identified (by arrows) as the temperature at which modulus begins to drop rapidly. The addition of SEP has two effects: a substantial increase in modulus (a filler effect) and a slight shift in the SI20 ordering transition (an interfacial ordering effect, see text).

SI20. At the boundaries between the SEP110-rich lamellae and either the SI20 droplet core or the SI20 external interface, the gray styrene microdomains of the respective phases are in contact (Figure 3B), as expected. The lamellae across the interface are therefore parallel to one another (Figure 3B).

When the molecular weight of the SI copolymer was increased, spherical SEP110-rich droplets no longer contained an SI core. Instead, more or less isolated SI100 lamellae were dispersed throughout the droplet (Figure 4) and arranged parallel to the SEP110 lamellae. Two types of SI100 lamellae are found within the SEP110-rich domains (Figure 4B): commensurate (labeled C) and inserted lamellae (unlabeled). In each case, the styrene microdomains of the SEP110 and SI100 lamellae are in contact. In the case of commensurate SI100 lamellae, the EP and I microdomains contact each other, whereas for inserted lamellae, they do not (Figure 4B). Inserted lamellae are more abundant (Figure 4B). In addition to these inclusions, the SEP110-rich lamellae again appear to contain dissolved SI100, and the interface, enriched in isoprene, is dark. Comparison of Figures 3B and 4B nevertheless indicates that the decoration of the interface in the latter case is less distinct, suggesting that the amount of SI100 that is dissolved within the SEP is somewhat less.

When the concentration of SEP is increased so that the SI-rich domains are the disperse phase, the SI droplets are not spherical, but scalloped in shape (Figure 5). The macrodomain interface follows the microdomain order of the SEP110-rich phase, which contains disclinations. These features apparently caused the notches mentioned before (Figure 2C). Presumably, these defects are created during macrophase separation so as to allow contact of the S microdomain, thereby reducing the interfacial tension between SI and SEP phases.

The influence of blending on the ODT of SI20 was examined rheologically. The ODT was detected as a marked decrease of the elastic modulus with increasing temperature (Figure 6).¹⁹ Pure SI20 was compared with blends containing 5 and 20 wt % SEP110. It was found

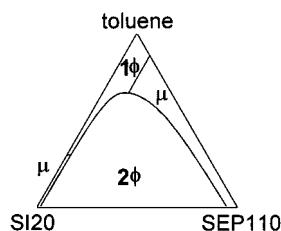


Figure 7. Schematic phase diagram of the ternary toluene/SI20/SEP110 system, illustrating single phase (1ϕ) disordered, two phase (2ϕ), and microphase (μ) states, as predicted qualitatively by mean-field theory.

that the ODT of the blend containing 5 wt % SEP110 was not significantly different than that for pure SI20 (Figure 6). On the other hand, the ODT of the blend containing 20 wt % SEP110 was measurably higher, by 3 °C (Figure 6). Optical microscopy investigations at elevated temperature demonstrated that the materials were macrophase separated and that droplets of SEP110-rich phase exist at both compositions. This testifies that the equilibrium concentration of SEP in the SI-rich phase is the same in both cases and therefore is quite small. Although we do not have a measurement of droplet size in the rheometer specimens, it is likely that the blend containing a larger volume of SEP110 also contained a larger interfacial area and had interfaces that are closer to one another. It is apparently this difference that contributed to the observed increase in the ODT. Although surface-induced order of block copolymers has been measured directly by X-ray and neutron reflectivity, the present instance is the first observation of a similar effect in bulk blends. Interfacially induced order is consistent with the morphological observation that the styrene microdomains of each phase are in contact with one another (Figure 3B).

Discussion

The sequence of transitions exhibited by these blends is qualitatively consistent with mean-field theory. Exact calculation is not possible because accurate segmental interaction parameters for these materials are not available. For styrene isoprene, several molecular weights have been investigated,²⁰ and for our materials a reasonable value of the interaction parameter seems to be $\chi_{SI} = -0.0013 + 16/T$.²⁰ For SI20, $\chi_{SI}N_{SI20} = 10.5$ at the order-disorder temperature of 147 °C, consistent with the Leibler prediction.⁴ At 22 °C, $\chi_{SI} = 0.053$. Assuming that toluene is neutral and that the critical value of $\chi_{SI,s}N = 10.5$, the order-disorder transition at 22 °C is predicted to occur at a polymer volume fraction of 0.70 for SI20 and of 0.14 for SI100. Sakurai et al.²¹ have obtained $\chi_{SEP} = 0.05 + 8/T$, which at 22 °C equals 0.077. Therefore, following the same assumptions, the order-disorder transition is predicted at a polymer volume fraction equal to 0.09. Due to the asymmetry of the SEP copolymer, however, the critical value of $\chi_{SEP,s}N_{SEP}$ may be greater than 10.5, thus shifting the transition to somewhat higher concentration. Reports of χ_{IEP} are not available, except for a report involving partially deuterated EP.²² Since the EP segments of the present report are fully hydrogenated, we assume a smaller value for $\chi_{IEP} = 0.02$. From eqs 1 and 4, we calculate χ_{eff} and N_{eff} to be 0.0103 and 565 and 0.0105 and 1511 for blends of SEP110 with SI20 and SI100, respectively. Using these values and assuming that the solvent is completely neutral, an approximate mean-field phase diagram was sketched (Figure 7). The

macrophase critical point for blends containing SI20 is predicted at a volume fraction of solids, $\phi_p = 0.34$, and a volume fraction of SEP110 relative to the amount of solids, $\phi_{SEP} = 0.30$. (For the higher molecular weight SI100, the critical point for macrophase separation is predicted under more dilute conditions, i.e., at $\phi_p = 0.13$.) Based upon Figure 7, blends that are rich in SEP110 are predicted to microphase separate before macrophase separation. On the other hand, blends that are rich in SI20 are predicted to macrophase separate and induce microphase ordering of the SEP-rich phase. These predictions are consistent with experimental observation (see discussion of Figure 2). Finally, note that the line defining the 1ϕ -to-microphase transition for blends rich in SEP110 is drawn nearly parallel to the left edge of the phase diagram, as a consequence of assuming that SI20 acts nearly as a neutral solvent, much like toluene. This assumption is based on the small size of SI20 relative to SEP110 and the relatively weak order at this transition.

In these experiments, macrophase separation produced phases that were not completely pure. Although we have not measured the amount of SI in the SEP phase, nor vice versa, the amount of SI dissolved in the SEP-rich phase seems to be appreciable as indicated by the SI decoration of the SEP microdomain interfaces, and the inclusions of SI within the SEP-rich phase suggest that the amount of SI dissolved in that phase is greater at early stages of phase separation (Figure 7), as expected from the screening effect of the toluene solvent. The lack of SEP inclusions in the SI-rich phase may indicate reduced solubility of SEP in SI. The reason for the solubility of SI in SEP may be that the I segments screen the interaction between S and EP.

In comparing blends containing SI20 with those containing SI100, we expect that SI20 will have greater solubility in SEP, because of its lower molecular weight. In addition, SI20 molecules should diffuse within the ordered SEP-rich phase more easily. Owing to this difference, the inclusions of SI20 within SEP can collect together more readily. Interestingly, inclusions of SI20 may have formed at the droplet center in order to reduce the curvature strain of lamellae there. Details of the processes of purification of the phases and the growth and ordering of the SI inclusion would be very interesting indeed. The mobility of SI100 within an ordered SEP-rich droplet is expected to be significantly less, consistent with the observation of many inclusions dispersed throughout the droplet. The nucleation of these individual lamellae may be a process similar to a microphase separation process in ABC triblock copolymers which at elevated temperatures form an ordered state in which two of the segments (A and C) are mixed and at lower temperatures separate.^{23,24} The motion of SI copolymers parallel or perpendicular to the lamellae may influence the incidence of commensurate or inserted lamellae.

Conclusions

Both macro- and microphase separation occur in these systems, and several factors determine their final morphology. The microdomain ordering and the macrodomain morphology influence each other. When macrophase separation occurs by nucleation and growth and induces microphase separation of droplets (SEP-rich), the droplets remain nearly spherical and the lamellae form concentric shells. However, when microphase separation precedes macrophase separation, the mac-

rod domain interface is severely distorted. In either case, the adjacent lamellae in neighboring phases are parallel and make contact through their styrene microdomains. Small domains of SI are also observed. When the mobility of the SI is restricted, isolated lamellae are nucleated. When the mobility of the SI is higher, the SI collect at the droplet center, a disclination core, apparently to relieve curvature strain of SEP lamellae.

The relative solubility of the components in each phase was determined qualitatively by microscopic and rheological analysis. The SI20 and SI100 are more soluble in SEP110 than is SEP in SI. The presence of SI within SEP was suggested by selective staining of the isoprene block at the microdomain interface between S and EP blocks. Although SEP is sufficiently insoluble in SI that it does not influence the ODT, its presence as a separate phase does elevate the ODT. This work is the first demonstration of interfacially induced ordering within a bulk block copolymer sample.

Acknowledgment. The partial support of NSF Grant NSF-CTS-9731502 is gratefully acknowledged.

References and Notes

- (1) Ohta, T. *J. Phys.: Condens. Matter* **1996**, *8*, A65–A80.
- (2) Stockmayer, W. H.; Moore, Jr., L. D.; Fixman, M.; Epstein, B. N. *J. Polym. Sci.* **1955**, *16*, 517–530.
- (3) tenBrinke, G.; Karasz, F.; MacKnight, W. J. *Macromolecules* **1983**, *16*, 1827.
- (4) Leibler, L. *Macromolecules* **1980**, *13*, 1602.
- (5) Fredrickson, G. H.; Helfand, E. *J. Chem. Phys.* **1987**, *87*, 697.
- (6) Kim, J. K.; Kimishima, K.; Hashimoto, T. *Macromolecules* **1993**, *26*, 125–136.
- (7) Roe, R.-J.; Zin, W.-C. *Macromolecules* **1984**, *17*, 189.
- (8) Hashimoto, T.; Tanaka, H.; Hasegawa, H. *Macromolecules* **1990**, *23*, 4378.
- (9) Tucker, P. S.; Barlow, J. W.; Paul, D. R. *Macromolecules* **1988**, *21*, 2794–2800.
- (10) Lowenhaupt, B.; Steurer, A.; Hellmann, G. P.; Gallot, Y. *Macromolecules* **1994**, *27*, 908–16.
- (11) Spontak, R. J.; Fung, J. C.; Braunfeld, M. B.; Sedat, J. W.; Agard, D. A.; Kane, L.; Smith, S. D.; Satkowski, M. M.; Ashraf, A.; Hajduk, D. A.; Gruner, S. M. *Macromolecules* **1996**, *29*, 4494.
- (12) Hashimoto, T.; Yamasaki, K.; Koizumi, S.; Hasegawa, H. *Macromolecules* **1993**, *26*, 2895–2904.
- (13) Lin, E. K.; Gast, A. P.; Shi, A. C.; Noolandi, J.; Smith, S. D. *Macromolecules* **1996**, *29*, 5920–5925.
- (14) Jeon, H. G.; Hudson, S. D.; Ishida, H.; Smith, S. D. *Macromolecules*, to be submitted.
- (15) Morton, M.; Fetters, L. J. *Rubber Chem. Technol.* **1975**, *48*, 359.
- (16) Bates, F. S.; Schulz, M. F.; Khandpur, A. K.; Forster, S.; Rosedale, J. H.; Almdal, K.; Mortensen, K. *Faraday Discuss.* **1994**, *7*–18.
- (17) Pinheiro, B. S.; Hajduk, D. A.; Gruner, S. M.; Winey, K. I. *Macromolecules* **1996**, *29*, 1482.
- (18) Scott, R. L. *J. Chem. Phys.* **1949**, *17*, 279–284.
- (19) Rosedale, J. H.; Bates, F. S. *Macromolecules* **1990**, *23*, 2329–2338.
- (20) Mori, K.; Okawara, A.; Hashimoto, T. *J. Chem. Phys.* **1996**, *104*, 7765–7777.
- (21) Sakurai, S.; Hashimoto, T.; Fetters, L. J. *Macromolecules* **1995**, *28*, 7947–7949.
- (22) Cumming, A.; Wiltzius, P.; Bates, F. S.; Rosedale, J. H. *Phys. Rev. A* **1992**, *45*, 885–897.
- (23) Chen, Z. R.; Kornfield, J. A.; Smith, S. D.; Grothaus, J. T.; Satkowski, M. M. *Science* **1997**, *277*, 1248–1253.
- (24) Chen, Z. R.; Kornfield, J. A., private communication, 1997.
- (25) **Note Added in Proof.** A similar observation concerning the structure of a lamellar phase comprising SI and SEP copolymers has been reported recently (Kimishima, K.; Jinnai, H.; Hashimoto, T., submitted to *Macromolecules*). In that report concerning 50/50 blends of SEP and SI copolymers, macrophase separation was suppressed by setting the fraction of polystyrene of both copolymers to be the same. Moreover, the interaction between the two copolymers was reduced by partial hydrogenation of the polyisoprene segment. Preferential segregation of isoprene segments to the interface between EP and S rich microdomains was observed.

MA9816665